# Proton and Hydride Transfers in Solution: Hybrid QM/MM Free Energy Perturbation Study.

L. Lawrence Ho,[†‡] Alexander D. MacKerell, Jr.,[¶] and Paul A. Bash[‡*]



[‡] *Center for Mechanistic Biology and Biotechnology*
*Argonne National Laboratory*
*Argonne, IL 60439*

[†] *J.W. Gibbs Laboratory*
*Department of Physics*
*Yale University*
*New Haven, CT 06511*

[¶] *Department of Pharmaceutical Sciences*
*School of Pharmacy*
*University of Maryland at Baltimore*
*Baltimore, MD 21230*



* To whom reprint requests should be addressed

**Abstract:** *A hybrid quantum and molecular mechanical (QM/MM) free energy perturbation (FEP) method is implemented in the context of molecular dynamics (MD). The semiempirical quantum mechanical (QM) Hamiltonian (Austin Model 1) represents solute molecules, and the molecular mechanical (MM) CHARMM force field describes the water solvent. The QM/MM FEP method is used to calculate the free energy changes in aqueous solution for (1) a proton transfer from methanol to imidazole and (2) a hydride transfer from methoxide to nicotinamide. The QM/MM interaction energies between the solute and solvent are calibrated to emulate the solute–solvent interaction energies determined at the Hartee–Fock 6–31G(d) level of* ab initio *theory. The free energy changes for the proton and hydride transfers are calculated to be 15.1 and –6.3 kcal/mol, respectively, which compare favorably with the corresponding experimental values of 12.9 and –7.4 kcal/mol. An estimate of the reliability of the calculations is obtained through the computation of the forward (15.1 and –6.3 kcal/mol) and backward (–14.1 and 9.1 kcal/mol) free energy changes. The reasonable correspondence between these two independent calculations suggests that adequate phase space sampling is obtained along the reaction pathways chosen to transform the proton and hydride systems between their respective reactant and product states.*

**Note:** the chemical formulae (**Chemical Formulae 1** and **2**) displayed on this page (p. 3) are printed separately for graphic reproduction on p. 27 and p. 28, respectively, of this manuscript.

## Introduction

We describe a computational procedure which combines a hybrid quantum and molecular mechanical (QM/MM) Hamiltonian with molecular dynamics (MD) and free energy perturbation (FEP) methods for the calculation of free energy changes in condensed phase systems. As an application of our QM/MM FEP method, we calculate the free energy changes for the following proton and hydride transfer reactions in water. The proton transfer reaction (**R1**) is:

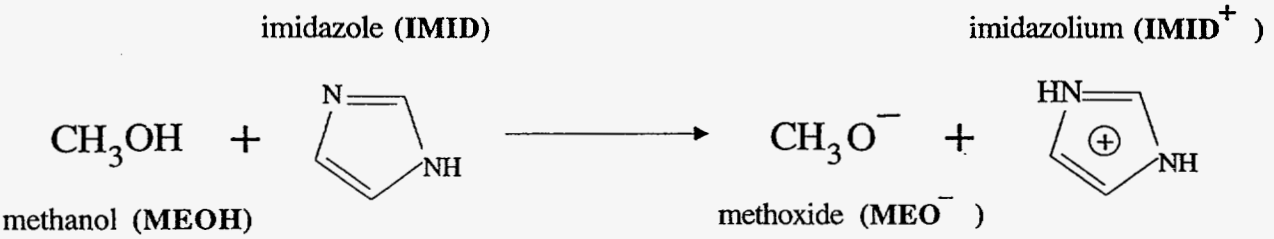


and the hydride transfer reaction (**R2**) is:

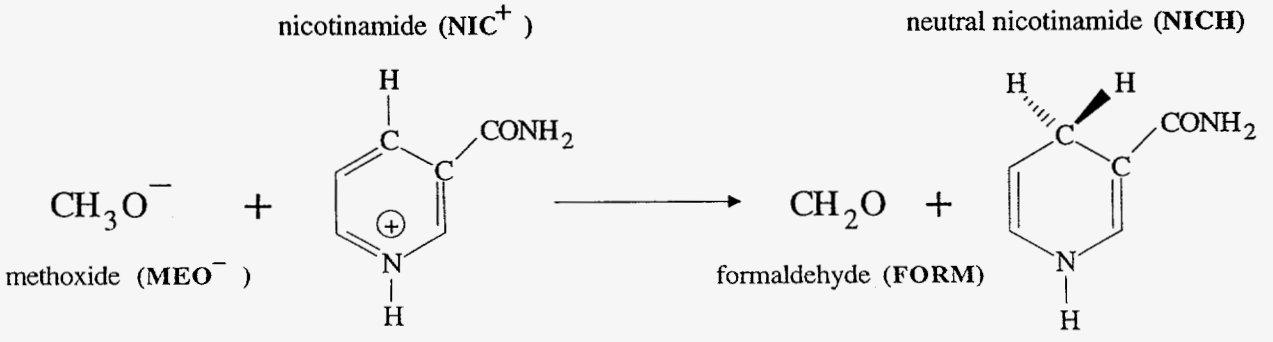


We chose the above molecular species for study because we are ultimately interested in simulating the reaction mechanism of the enzyme malate dehydrogenase (MDH), which interconverts malate and oxaloacetate through one proton and one hydride transfer in the citric acid cycle.[1-3] The biochemical reactions in MDH consist of a proton transfer from the hydroxyl group of malate to the imidazole side

chain of an active site histidine residue in the enzyme, and a hydride transfer from malate to the nicotinamide group of the enzyme co-factor nicotinamide adenine dinucleotide (NAD). The molecules designated as MEOH, IMID, $MEO^-$, $IMIDH^+$, $NIC^+$, and NICH in the reactions **R1** and **R2** are molecular analogues of functional groups that participate directly in the MDH reaction.

The motivation behind the simulations reported in this article is twofold. First, we intend to optimize and test the ability of our QM/MM FEP method to calculate the energetics and solvation effects for proton and hydride transfer reactions in aqueous solution. Reactions **R1** and **R2** are good test cases for evaluating the ability of our QM/MM FEP method to calculate reaction free energy changes because reliable free energies of transfer can be estimated from experimental pKa's and redox potentials.[4,5] Second, the free energy properties of these reactions in solution provide a standard from which we can calibrate our QM/MM FEP method for subsequent simulations of proton and hydride transfers in the protein-and-water environment of malate dehydrogenase. Once we have optimized the performance and established the accuracy of our QM/MM FEP method with respect to free energies of proton and hydride transfers in water, the free energy calculations of proton and hydride transfers in the context of malate dehydrogenase can then be more meaningfully interpreted.

The structure of this paper is as follows. First, we describe the QM/MM FEP method. Second, we report the energetic accuracy of the QM part of our QM/MM Hamiltonian, and we summarize the calibration of QM/MM interaction energies against *ab initio* calculations and experimental data. Third, we report the simulation details and interpret the results of our free energy calculations of proton and hydride transfers in water. We conclude with a discussion of our results and their implications for future research.

**QM/MM Free Energy Procedure**

We have previously developed a combined QM (semiempirical AM1)[6] and MM (CHARMM)[7] approach (QM/MM) for the study of condensed phase reactions, which extended and enhanced the concepts and implementations of earlier efforts.[8,9] To use a QM/MM method, a simulation system is partitioned into QM and MM regions. The energies $(E_{QM/MM})$ of and the forces $(\mathbf{F}_{QM/MM})$ on QM atoms are given by the expectation values of the QM Hamiltonian and its derivative, respectively, and include electrostatic and van der Waals interactions with MM atoms. The determination of $\mathbf{F}_{QM/MM}$ and $\mathbf{F}_{MM}$, the forces on MM atoms (which include effects due to QM atoms), enables energy minimization and classical molecular dynamics (MD) to be done in a standard manner.[10] With this QM/MM MD method, we can calculate ensemble–averaged thermodynamic quantities such as the free energy changes of proton and hydride transfer reactions. The power of this QM/MM approach in studying complex condensed phase reactions has been demonstrated by simulations of reaction pathways in solution[11-13] and by the simulation analysis of the enzyme reaction in triosephosphate isomerase, where a novel mechanism was suggested[14] and subsequently verified by experiment.[15]

To calculate the free energies of proton and hydride transfers in solution, we adopted a procedure similar in principle, but different in implementation, to that used by Gao[13] for the determination of the free energy profile of an $S_N2$ reaction in aqueous solution. We use free energy perturbation (FEP) theory implemented with molecular dynamics to calculate the potential of mean force along a reaction coordinate, which is defined as the distances between a donor or acceptor (carbon, nitrogen, or oxygen) and the transferring proton or hydride anion.

The free energy difference between two states, *A* and *B*, in thermodynamic equilibrium is

$$\Delta G(A \rightarrow B) = -RT \ln\left\langle \exp\left\{-[H(B) - H(A)]/RT\right\}\right\rangle_A , \qquad (1)$$

where $R$ and $T$ are the universal gas constant and absolute temperature, respectively, $H(A)$ and $H(B)$ are the Hamiltonians of states $A$ and $B$, and $\langle\ \rangle_A$ denotes an ensemble average calculated with respect to the probability density of state $A$. In practice, $\Delta G$ can be efficiently computed through the use of free energy perturbation (FEP) methods.[16]

In the FEP formalism, a system is characterized by a Hamiltonian $H(\boldsymbol{p},\boldsymbol{q};\lambda)$, which depends parametrically on a multidimensional coupling parameter $\lambda$ and is a function of phase space coordinates $\boldsymbol{p}$ and $\boldsymbol{q}$. The free energy difference between two states $A$ and $B$ can be calculated by the following procedure. First, a discrete pathway consisting of $N$ intermediate states $\lambda_i$ $(1 \le i \le N$ such that $A \equiv \lambda_1 \le \lambda_i \le \lambda_N \equiv B)$ is constructed to connect states $A$ and $B$. These intermediate states are referred to as free energy perturbation windows, or simply as the "windows". Second, free energy differences between neighboring states along the pathway are calculated by Equation 1. The free energy differences between a state $\lambda_i$ and its two neighbors $\lambda_{i\pm1} = \lambda_i \pm \Delta\lambda$ are

$$\Delta G_i(\lambda_i \rightarrow \lambda_i \pm \Delta\lambda) = -RT \ln\left\langle \exp\left\{-\left[H(\lambda_i \pm \Delta\lambda) - H(\lambda_i)\right]/RT\right\}\right\rangle_{\lambda_i}. \qquad (2)$$

Finally, the free energy changes of all intermediate perturbation windows along the pathway are summed to obtain the free energy difference between states $A$ and $B$, i.e.,

$$\Delta G(A \rightarrow B) = \sum_{i=1}^{N-1} \Delta G_i(\lambda_i \rightarrow \lambda_i + \Delta\lambda), \qquad (3)$$

$$\Delta G(B \rightarrow A) = \sum_{i=1}^{N-1} \Delta G_{N-i+1}(\lambda_{N-i+1} \rightarrow \lambda_{N-i+1} - \Delta\lambda). \qquad (4)$$

In practice, the number of perturbation windows ($N$) is chosen so that the phase space of the three states represented by $\lambda_i$, and $\lambda_i \pm \Delta\lambda$ can be adequately sampled. A value of $\Delta\lambda$ is chosen such that the probability densities of the two neighboring states $\lambda_i$ and $\lambda_i + \Delta\lambda$ (or $\lambda_i - \Delta\lambda$) are similar and that sufficient sampling will be obtained with respect to the probability density of state $\lambda_i$. For our proton

(hydride) transfer simulations, the perturbation coordinate $\lambda_{proton}$ ($\lambda_{hydride}$) is two-dimensional and consists of (1) the distance between the donor atom and the proton (hydride) and (2) the distance between the acceptor atom and the proton (hydride). Because the free energy is a state function for a thermodynamic system in equilibrium, the free energy change between states *A* and *B* is path-independent. Because we are only interested in calculating the free energy changes between states *A* and *B*, $\lambda_{proton}$ (or $\lambda_{hydride}$) can be arbitrarily chosen to connect the proton and hydride reactant and product states. In practice, we selected computationally efficient pathways which connect reactants *A* and products *B*.

**QM/MM Calibration**

Three factors determine the accuracy of our QM/MM FEP method: first, the ability of the QM part of the QM/MM Hamiltonian to accurately model the intrinsic energetic and structural properties of reactant and product states; second, the adequacy of the QM/MM Hamiltonian in reproducing the energetic effects of the solvent environment; and third, the ability of molecular dynamics to sample phase space sufficiently to obtain meaningful time–averaged thermodynamic quantities such as free energy changes. In this section, we address issues related to the energetic accuracy of the QM/MM Hamiltonian. Problems of phase space sampling will be discussed later.

The theoretical and experimental absolute heats of formation ($\Delta H_f^0$) of the various molecular species that constitute our proton and hydride transfer reactions are displayed in Table 1. The AM1–derived $\Delta H_f^0$ differ by as much as 20 kcal/mol from their experimental counterparts for the proton transfer reaction. However, for proton transfer free energy change calculations, only the relative enthalpy of reaction, i.e., $\Delta\Delta H_r^0(proton) = \Delta H_f^0(IMIDH) + \Delta H_f^0(MEO) - \Delta H_f^0(IMID) - \Delta H_f^0(MEOH)$, is relevant. In this instance, the calculated $\Delta\Delta H_r^0(proton)$ = 164.1 kcal/mol overestimates the experimental $\Delta\Delta H_r^0(proton)$ = 157 kcal/mol by only 7 kcal/mol, which is within 4 % of the total proton transfer enthalpy. For the hydride transfer reaction, the experimental $\Delta H_f^0$ value of NIC and NICH are not available. Hence, the inherent accuracy of AM1 in this case can not be determined directly. An evaluation

of the adequacy of AM1 in the context of the energetics of the hydride transfer reaction in aqueous solution must await the final results of our solution free energy calculations, where we will provide an *a posteriori* justification of the adequacy of AM1 in modeling hydride transfer energetics. The calculated $\Delta\Delta H_r^0$ for reaction **(R2)** is $-158$ kcal/mol.

The above gas phase calculations provide an estimate of the inherent accuracy of the AM1 method in modeling the energetics of these proton and hydride reactions. However, we are interested primarily in evaluating the ability of our QM/MM FEP method to model the energetics and solvation effects in condensed phase reactions. To model solvation effects realistically, it is necessary that the QM/MM Hamiltonian represents as accurately as possible the interaction energies between solute atoms (which are described by QM) and solvent atoms (which are described by MM). In our QM/MM method, QM and MM atoms interact through (1) the one-electron Hamiltonian via QM electron and MM "core" partial charges, (2) QM core positive charges and MM "core" partial charges, and (3) QM and MM van der Waals (vdW) interactions. Term (3) models electronic repulsion and dispersion interactions, which do not exist between QM and MM atoms because MM atoms possess no explicit electrons. Within the framework of this formalism, QM/MM interactions can be calibrated by adjusting the vdW parameters of QM atoms such that the interaction energies between QM and MM atoms emulate those determined from *ab initio* QM calculations and experimental data.

Our QM/MM interaction energy optimization procedure is similar in principle to one used to develop a molecular mechanics force field.[17] Specifically, we match the interaction energy between a water molecule (MM) and a functional group (QM) calculated by our QM/MM Hamiltonian to those determined at the Hartree-Fock 6-31G(d) level of theory. This fitting procedure is accomplished by adjusting the vdW parameters of the QM atoms until the QM/MM interaction energies agree with the *ab intio* values. The 6-31G(d) basis set has been shown to reproduce interaction energies for hydrogen bonding complexes with good accuracy,[18,19] and therefore provides a reasonable standard for our QM/MM calibrations.

To calculate the interaction energies between water (MM) and solute (QM), we used the following procedure. First, the geometry of each model compound monomer, including the water probe, was optimized using Gaussian HF 6-31G(d), AM1, and MM levels of theory. Using these optimized monomers, model compound/water complexes were constructed in the orientations shown in Figure 1. All degrees of freedom were fixed except the distance and/or angle parameters shown in these figures, which were optimized to obtain the minimum energy conformations of each complex with respect to the given set of constraints. Table 2 lists the *ab initio* interaction energies scaled by a factor of 1.16 for uncharged molecules, because it has been determined that 6-31G(d) interaction energies scaled by a factor of 1.16 provides a more realistic standard than the native *ab initio* values for neutral molecules.[20] The vdW parameters (Table 3) on the AM1 QM atoms of molecules IMIDH, $NIC^+$ , and $MEO^-$ were adjusted so that the QM/MM interaction energies emulate as closely as possible the *ab initio* interaction energies. These vdW parameters were then used on analogous atom types in IMID, NICH, and FORM. Satisfactory agreement between *ab initio* and QM/MM interaction energies was found. The average deviation of these QM/MM interaction energies from the *ab initio* reference values was $0.42 \pm 0.44$ kcal/mol. However, the interaction distance between AM1 QM and MM water probe was generally too short by $0.25 \pm 0.14$ Å when compared to the *ab initio* values. The largest deviations were between 0.3 and 0.5 Å for $MEO^-$ , MEOH, and FORM. Although these are relatively large structural errors for these complexes, our primary interest is the simulation of the energetic properties of these molecules in bulk aqueous solution. With respect to this objective, the interaction energies are more important and we concentrated our effort on the fitting of the interaction energies to be as close as possible to *ab initio* values at the expense of some error in the structures of the complexes. These results are similar to those obtained by Gao.[21]

**Proton Transfer and Hydride Transfer Free Energy Calculations**

Two reaction coordinates are used to describe both the proton and hydride transfer reactions. Schematic diagrams of the proton and hydride transfer solutes and their corresponding reaction coordinates are displayed in Figures 2 and 3, respectively. For FEP calculations, the two-dimensional coupling constants for proton and hydride transfer are $\lambda_{proton} \equiv \{d(O2-H2), d(H2-NE2)\}$, and $\lambda_{hydride} \equiv \{d(C2-H21), d(H21-C4N)\}$, where $d(X-Y) \equiv$ "distance between atoms $X$ and $Y$".

We modeled the proton and hydride reactions in solution as follows. The solute molecules represented in Figures 2 and 3 are immersed in 18-Å radius balls of TIP3P water[22] centered at atom CG (IMID and $IMIDH^+$) for the proton system and atom NA ($NIC^+$ and NICH) for the hydride system. We removed all TIP3P molecules within 3.1 Å of nonhydrogen solute atoms. A deformable stochastic boundary[23,24] with a reaction zone of 16 Å and a buffer region of 2 Å was imposed on both proton and hydride reaction systems, and molecular dynamics was used to sample phase space. The atom CG (Figure 2) in the proton system and atom N2 (Figure 3) of the hydride system were fixed in space. All other degrees of freedom were unconstrained except the reaction coordinates $\lambda_{proton}$ and $\lambda_{hydride}$, which were constrained using SHAKE[25], to specific values along the FEP pathways (for numerical values of $\lambda_i$, see Tables 4 and 5). The initial geometry of the carbonyl oxygen in the protonated nicotinamide was *trans* to atom C4N (as shown in Figure 3).

To calculate the free energies for the proton or the hydride transfer, two states $A$ (reactant state) and $B$ (product state) are defined with a set of reaction coordinates ($\lambda_{proton}$ or $\lambda_{hydride}$), and each system is transformed from state $A$ to state $B$ along a convenient pathway. For the proton transfer system, the reaction pathway consisted of a series of changes in the two reaction coordinates $d(O2-H2)$ and $d(H2-NE2)$ (0.05 Å increments) such that the system was transformed from a methanol-imidazole

complex to a methoxide-imidazolium complex. Three partitions are defined along the pathway as (1) the proton transfer region, (2) MEOH complex region, and (3) $MEO^-$ complex region. The proton transfer region is defined by perturbation windows where the proton is transferred from MEOH to IMID by alternately changing the distances $d(O2-H2)$ and $d(H2-NE2)$ while keeping their sum, $d(O2-H2)+d(H2-NE2)$, to 2.45 or 2.50 Å (see Table 4). In the MEOH complex region, $d(H2-NE2)$ is altered from 1.45 to 3.0 Å while $d(O2-H2)$ is kept constant at 1.0 Å. The $MEO^-$ complex region consists of perturbation windows where $d(O2-H2)$ changes from 1.45 to 2.45 Å and $d(H2-NE2)$ is kept constant at 1.0 Å. The end points for the $MEO^-$ and MEOH complex regions were defined where the calculated free energy changes approached values close to zero (Table 4 and Figure 4). The reaction pathway for the hydride transfer reaction was determined by an analogous procedure.

For each window in the above pathways, either $d(O2-H2)$ [$d(C2-H21)$ in the hydride case] or $d(H2-NE2)$ [$d(H21-C4N)$ in the hydride case] was perturbed, but not both. To perturb the reaction coordinate $d(O2-H2)$, the atom H2 is included in the definition of molecule IMID and reaction coordinate $d(H2-NE2)$ is held constant. The two molecules, MEO and IMID, are subsequently displaced as rigid bodies along the vector defined by the O2-H2 bond by ±0.025 Å, which produces a net change in the O2-H2 bond length of ±0.05 Å. A similar procedure is used to perturb the reaction coordinate $d(H2-NE2)$. In this case, H2 is included in the definition of molecule $MEO^-$, and the perturbation is along the vector defined by the H2–NE2 bond (Figure 2). The hydride transfer reaction coordinates are transformed by an analogous protocol.

To illustrate the computational details, we use the proton transfer system. A pre-equilibration of one starting window ($\lambda_{proton} \equiv \{d(O2\text{-}H2) = d(H2\text{-}NE2) = 1.3$ Å$\}$) was carried out for 80 ps using 1-fs time steps at a constant temperature of 298 K. The solute molecules are treated with QM and solvent with MM for all equilibration and data collection simulations. The coordinates and velocities from the end of this pre-equilibration MD run were used as the initial conditions for subsequent MD simulations defined in

Table 4. These perturbation windows are physically independent of one another, and simulations associated with these states can therefore be done in parallel. The equilibration and data collection tasks of each window were assigned to separate processors of a 128-node IBM SP parallel computer. To ensure that each of these independent systems and simulations was adequately equilibrated, an additional 20 ps of MD at 298 K was run for each window. After this equilibration phase, 10 ps of free energy data collection was carried out. The data displayed in Table 4 shows that the free energy change of each window after 5 ps of data collection is very close to that after 10 ps. This suggests that adequate equilibration had been attained for all perturbation windows and that the calculated free energies had converged.

For each proton perturbation window, we calculated the free energy changes for the "forward" and "backward" directions ($\lambda_i$ to $\lambda_i \pm \Delta\lambda$), which is known as "double-wide sampling" (Equation 2). The total free energy changes $\Delta G_{proton}(forward)$ and $\Delta G_{proton}(backward)$ are determined using Equations 3 and 4, respectively. An estimation of the hysteresis associated with each window is

$$\Delta G_{proton,i}(hystersis) = \left|\Delta G_i(\lambda_{proton,i} + \Delta\lambda) - \Delta G_i(\lambda_{proton,i} - \Delta\lambda)\right| \quad (5)$$

and the total hysteresis is

$$\Delta G_{proton}(hystersis) = \left|\Delta G_{proton}(forward) - \Delta G_{proton}(backward)\right| \quad (6)$$

The total hysteresis for the proton transfer simulations is about 1 kcal/mol, which suggests that adequate phase space sampling had been achieved along the entire pathway. A plot of the free energy changes for the forward and backward directions, which are listed in Table 4, is shown in Figure 4.

The calculations of the free energy changes associated with the hydride transfer reaction were carried out using a procedure analogous to that used for the proton transfer reaction. As in the proton case, a comparison between 5 ps and 10 ps of data collection suggests that the free energy values have converged. However, the hysteresis in the calculated total free energies is 2.8 kcal/mol, which is higher than the value obtained for the proton transfer calculations and suggests insufficient sampling may have occurred in some regions along the pathway. A closer look at Table 5 shows that all of the hysteresis is accumulated in the portion of the pathway where the hydride is actually transferred between the donor and acceptor atoms (i.e., windows where $d(C2-H21)+d(H21-C4N)=$ 2.65 or 2.70 Å). A visual inspection of representative molecular geometries from the MD trajectories associated with these windows indicated that rotation of the amide and carbonyl groups about the C9–C12 bond (see Figure 1) of the nicotinamide occurred during the course of these simulations and that the dihedral angle C4N–C9–C12–O13 differs from one window to another. This leads to the observed hysteresis, which may be reduced by adopting a smaller perturbation increment, $\Delta\lambda$, and/or performing more phase space sampling in this region of our pathway. The free energy results for the hydride transfer simulations are shown in Table 5 and Figure 5.

**Discussion**

In the condensed phase, solvation effects can dramatically alter the energetics of chemical reactions, and our free energy simulations illustrate this point. The energy required to transfer a proton from methanol to imidazole in vacuum, depicted in reaction **R1**, is about 157 kcal/mol (Table 1), whereas, the experimental free energy for this proton transfer in water at 298 K is only 12.9 kcal/mol. This solution value is calculated from the experimental $pK_a$'s of methanol (15.5)[4] and imidazole (6.04)[26] where $\Delta G_{solvent}(\mathbf{R1}) = 2.3RT\{-pK_a(\mathbf{IMID}) - pK_a(\mathbf{MEOH})\}$. There is a significant energetic stabilization effect due to the solvation of methoxide (charge $-1$) and imidazolium (charge $+1$) relative to the uncharged methanol and imidazole species, which is due to the electrostatic screening and hydrogen-bonding properties of water. Our simulated proton free energy change (Table 4 and Figure 4) of 15.1 kcal/mol (–14.2 for the backward transformation) compares favorably to the experimental value of 12.9

kcal/mol and appears to account for most of the effects of solvation. The good agreement between theory and experiment in this case is due to (1) the ability of AM1 to reproduce sufficiently well the $\Delta\Delta H_r^0$ of reaction **R1**, (2) the calibration of QM/MM interaction energies which lead to a reasonable representation of solvation energetics, and (3) the adequate sampling of phase space along the pathway chosen for the perturbations as obtained through the MD simulations.

An experimental value for a hydride transfer from $MEO^-$ to $NIC^+$ is not available. However, using the standard redox potentials[5] of a similar set of molecules (ethanol, acetaldehyde, NAD, and NADH) as the ones used in our simulations, the free energy change, $\Delta G_{solvent}(\mathbf{R3})$, of the reaction

$$MEOH + NIC^+ \rightarrow FORM + NICH \qquad \textbf{(R3)}$$

is estimated to be 5.5 kcal/mol. Using the principle of thermodynamic cycles, the free energy change, $\Delta G_{solvent}(\mathbf{R2})$, for the hydride transfer reaction **R2** is determined from $\Delta G_{solvent}(\mathbf{R2}) = \Delta G_{solvent}(\mathbf{R3}) - \Delta G_{solvent}(\mathbf{R1})$ = 5.5 kcal/mol – 12.9 kcal/mol = –7.4 kcal/mol. We obtained a simulated $\Delta G_{solvent}(\mathbf{R2})$ value of –6.3 kcal/mol for the forward direction and 9.1 kcal/mol in the reverse direction (Table 5 and Figure 5). Our calculated values compare reasonably well with the estimated experimental free energy change for this hydride transfer reaction in solution. Solvation effects can be obtained by comparing gas phase and solution energy changes for reaction **R2**. Experimental heats of formation for protonated nicotinamide and 1,4dihydronicotinamide are not available, therefore, we use the AM1 values for comparison to the solution calculations. From the experimentally derived value of $\Delta G_{solvent}(\mathbf{R2})$ = –7.4 kcal/mol and the AM1 calculated $\Delta\Delta H_r^0(\mathbf{R2})$ = –158 kcal/mol, the water solvent is estimated to stabilize the charged reactants with respect to the uncharged products by about 150 kcal/mol. Our calculated and experimentally derived values for $\Delta G_{solvent}(\mathbf{R2})$ are within 2 kcal/mol of each other, which suggests that we are including the stabilization effects of the solvent environment reasonably well. These results, together with those of the proton transfer simulations, indicate that our AM1 QM/MM

method provides a good model for the energetics of these particular functional groups in the context of a water solvent condensed phase.

## Conclusions

We have described the theoretical principles and computational implementations of a hybrid quantum and molecular mechanical free energy perturbation method, which can be used to simulate the properties of condensed phase reactions. This method uses molecular dynamics to generate statistical ensembles, which lead to time-averaged quantities such as the free energy. We have demonstrated that when the QM/MM Hamiltonian is calibrated to reproduce the solvation effects of a water molecule (which is described by molecular mechanics) interacting with a solute molecule (which is described by quantum mechanics), the QM/MM FEP method can calculate the free energy changes for proton and hydride transfers in solution to almost experimental accuracy. The quality of the performance of the QM/MM FEP method in these sets of simulations can be attributed to two factors. First, the AM1 Hamiltonian models the relative heats of formation for the gas phase reactions **R1** and **R2** with reasonable accuracy. Second, solvation effects dominate in both the proton and hydride transfer reactions, which we are able to emulate through our QM/MM solvent parameterization procedure.

In addition to demonstrating the viability of our QM/MM FEP method in describing proton and hydride transfers in solution, this study paves the way for the simulation and analysis of the reaction mechanism in the enzyme malate dehydrogenase. For malate dehydrogenase, the functional groups involved in its proton and hydride transfer reactions are analogous to the solute molecules used in this study. We anticipate that the amino acid solvent environment of the enzyme will dominate the energetics associated with its proton and hydride transfers. The vdW parameters obtained in the present set of calibrations of solute (QM) and water (MM) interactions should provide a reasonable first approximation to the vdW parameters to be used in the enzyme (MM) and reaction zone (QM) simulations of proton and hydride transfers in malate dehydrogenase.

**Acknowledgments**

The authors gratefully acknowledge use of the Argonne High-Performance Computing Research Facility. The HPCRF is funded principally by the U.S. Department of Energy Office of Scientific Computing. This work was also supported by the U.S. Department of Energy Office of Health and Environmental Research, under Contract no. W-31-109-Eng-38.

## References


(1) Hall M.D. and Banaszak L.J. *J. Mol. Biol.* **1993**, 232, 213.

(2) Parker D.M.; Lodola A.; Holbrook J.J. *Biochem. J.* **1978**, 173, 959-967.

(3) Lodola A.; Shore J.D.; Parker D.M.; Holbrook J. *Biochem. J.* **1978**, 175, 987-998.

(4) Maskill H., *The Physical Basis of Organic Chemistry*; Oxford University Press: New York, 1989.

(5) Fasman P.A., *Handbook of Biochemistry and Molecular Biology*; CRC Press: Cleveland, 1976.

(6) Dewar M.J.S. and Zoebisch E.G. *J. Am. Chem. Soc.* **1985**, 107, 3902.

(7) Brooks B.; Bruccoleri R.E.; Olafson B.; States D.J.; Swaminathan S.; Karplus M. *J. Comp. Chem.* **1983**, 4, 187.

(8) Warshel A. and Levitt M. *J. Mol. Biol.* **1976**, 103, 227.

(9) Singh U.C. and Kollman P.A. *J. Comp. Chem.* **1986**, 7, 718.

(10) Brooks C.L. III; Karplus M.; Pettitt B.M., *Proteins: A Theoretical Perspective of Dynamics, Structure, and Thermodynamics* (*Adv. Chem. Phys. LXXI*); John Wiley & Sons: New York, 1988.

(11) Bash P.A.; Field M.J.; Karplus M. *J. Amer. Chem. Soc.* **1987**, 109, 8092.

(12) Gao J.L. and Xia X.F. *Science* **1992**, 258, 631-635.

(13) Gao J. and Xia X. *J. Am. Chem. Soc.* **1993**, 115, 9667.

(14) Bash P.A.; Field M.J.; Davenport R.; Ringe D.; Petsko G.; Karplus M. *Biochemistry* **1991**, 30, 5826.

(15) Knowles J.R. *Nature* **1991**, 350, 121.

(16) Bash P.A.; Singh U.C.; Langridge R.; Kollman P.A. *Science* **1987**, 236, 574.

(17) MacKerell A.D.; Bashford D.; Bellot M.; Dunbrack R.L.; Field M.J.; Fischer S.; Gao J.; Guo H.; Ha S.; Joseph D.; Kuchnir L.; Kuczera K.; Lau F.T.K.; Mattos C.; Michnick S.; Ngo T.; Nguyen D.T.; Prodhom B.; Roux B.; Schlenkrich M.; Smith J.C.; Stote R.; Straub J.; Wiorkiewicz-Kuczera J.; Karplus M. *FASEB Journal* **1992**, 6, A143.

(18) Hehre W.J.; Radom L.; Scheyer P.; Pople J.A., *Ab Initio Molecular Oribital Theory*; John Wiley & Sons: New York, 1986.

(19) Pranata J.; Wierschke S.G.; Jorgensen W.L. *J. Am. Chem. Soc.* **1991**, 113, 2810.

(20) MacKerell A.D. and Karplus M. *J. Phys. Chem.* **1991**, 95, 10559-10560.

(21) Gao J. In *Modeling the Hydrogen Bond*; Smith D.A., Eds.; ACS Symp. Series 569, 1994.

(22) Jorgensen W.L.; Chandrasekhar J.; Madura J.; Impey R.W.; Klein M.L. *J. Chem. Phys.* **1983**, 79, 926.

(23) Brooks III C.L. and Brünger A. *Biopolymers* **1985**, 24, 843.

(24) Brooks III C.L. and Karplus M. *J. Mol. Biol.* **1989**, 208, 159-181.

(25) van Gunsteren W.F. and Berendsen H.J.C. *Mol. Phys.* **1977**, 34, 1311.

(26) Dawson R.M.C.; Elliot D.C.; Elliot W.H.; Jones K.M., *Data for Biochemical Research*; Oxford University Press: New York, 1986.

(27) Lias S.G.; Bartmess J.E.; Liebman J.F.; Holmes J.L.; Levin R.D.; Mallard W.G., *Gas-Phase Ion and Neutral Thermochemistry, J. Phys. & Chem. Ref. Data* **1988**, 17 (Suppl. 1).

(28) Meot-Ner M. and Sieck L.W. *J. Phys. Chem.* **1986**, 90, 6687-6690.

## Table 1

| *Molecular Group* **(Solute)** | *AM1* $\Delta H_f^\phi$ *(kcal/mol)* | *Experimental* $\Delta H_f^\phi$ *(kcal/mol)* |
|---|---|---|
| **MEO** | –38.52 | –33.1±2.9 |
| **MEOH** | –57.06 | –48.1 |
| **IMID** | 50.76 | 35.0±0.5 |
| **IMIDH** | 196.31 | 177.0 |
| **FORM** | –31.52 | –26.0±0.2 |
| **NIC** | 150.14 | — |
| **NICH** | –14.69 | — |

**Table 1.** Semiempirical QM (AM1) and experimental absolute heats of formation ($\Delta H_f^\phi$)[27] of solute molecules used in the proton and hydride transfer reactions.

**Table 2**

| Molecule | 6-31G* | | AM1/MM | | MM | |
|---|---|---|---|---|---|---|
| *(orientation)* | *Energy* | *d(OW–X) (angle)* | *Energy* | *d(OW–X) (angle)* | *Energy* | *d(OW–X) (angle)* |
| **IMID (1)** | -2.44 | 3.45 (CE) | -2.58 | 3.24 (CE) | -2.43 | 3.22 (CE) |
| **IMID (2)** | -7.26 | 3.12 (NE2) | -6.62 | 2.80 (NE2) | -6.95 | 2.90 (NE2) |
| **IMID (3)** | -0.99 | 3.66 (CD) | -0.57 | 3.68 (CD) | -0.87 | 3.64 (CD) |
| **IMID (4)** | -2.40 | 3.51 (CG) | -1.63 | 3.62 (CG) | -1.48 | 3.66 (CG) |
| **IMID (5)** | -6.65 | 3.07 (ND) | -6.39 | 2.80 (ND) | -6.54 | 2.88 (ND) |
| **IMIDH (1)** | -12.28 | 3.03 (CE) | -12.66 | 2.94 (CE) | -12.28 | 2.94 (CE) |
| **IMIDH (2)** | -9.53 | 3.13 (CD) | -9.26 | 3.12 (CD) | -9.48 | 3.12 (CD) |
| **IMIDH (3)** | -15.94 | 2.85 (ND) | -16.10 | 2.68 (ND) | -16.09 | 2.76 (ND) |
| **NICH (1)** | -2.95 | 3.68 (N14) | -2.70 | 3.14 (N14) | — | — |
| **NICH (2)** | -4.10 | 3.11 (N14) | -4.11 | 2.82 (N14) | — | — |
| **NICH (3)** | -1.51 | 3.76 (C4N) | -0.95 | 3.30 (C4N) | — | — |
| **NICH (4)** | -1.18 | 3.70 (C4N) | -0.94 | 3.30 (C4N) | — | — |
| **NICH (5)** | -1.40 | 3.73 (C5) | -1.18 | 3.30 (C5) | — | — |
| **NICH (6)** | -2.42 | 3.55 (C3) | -2.43 | 3.20 (C3) | — | — |
| **NICH (7)** | -6.11 | 3.10 (N2) | -6.04 | 2.82 (N2) | — | — |
| **NICH (8)** | -1.22 | 3.32 (C10) | -1.32 | 3.28 (C10) | — | — |
| **NICH (9)** | -8.93 | 2.94 (O13) (θ=141) | -9.05 | 2.74 (O13) (θ=140) | — | — |
| **NICH (10)** | -9.03 | 3.05 (O13) (ϕ=117) | -8.20 | 2.76 (O13) (ϕ=120) | — | — |
| **NIC (1)** | -8.92 | 3.37 (N14) | -8.91 | 3.00 (N14) | -8.94 | 3.11 (N14) |
| **NIC (2)** | -9.64 | 2.95 (N14) | -9.80 | 2.74 (N14) | -9.63 | 2.85 (N14) |
| **NIC (3)** | -10.02 | 3.30 (C4N) | -9.80 | 3.02 (C4N) | -10.04 | 3.17 (C4N) |
| **NIC (4)** | -8.60 | 3.19 (C5) | -8.69 | 3.04 (C5) | -8.54 | 3.15 (C5) |
| **NIC (5)** | -10.50 | 3.11 (C3) | -10.58 | 3.00 (C3) | -10.50 | 3.11 (C3) |
| **NIC (6)** | -16.58 | 2.84 (N2) | -16.91 | 2.68 (N2) | — | — |
| **NIC (7)** | -9.11 | 3.05 (C10) | -8.88 | 3.14 (C10) | -9.18 | 3.13 (C10) |
| **NIC (8)** | -5.56 | 2.98 (O13) (θ=141) | -7.31 | 2.76 (O13) (θ=135) | -5.66 | 2.80 (O13) (θ=140) |
| **NIC (9)** | -3.64 | 3.05 (O13) (ϕ=108) | -4.28 | 2.80 (O13) (ϕ=110) | -3.41 | 2.88 (O13) (ϕ=101) |
| **MEO (1)** | -18.75 | 2.67 (O2) | -20.17 | 2.38 (O2) | -20.33 | 2.62 (O2) |
| **MEO (2)** | -20.95 | 2.70 (O2) | -21.43 | 2.44 (O2) | -21.25 | 2.58 (O2) |
| **MEO (3)** | -20.95 | 2.70 (O2) | -21.43 | 2.44 (O2) | -21.26 | 2.58 (O2) |
| **MEO (4)** | -23.96 | 2.71 (O2) (θ=115) | -23.96 | 2.46 (O2) (θ=132) | -23.34 | 2.64 (O2) (θ=98) |
| **MEO (5)** | -6.89 | 2.47 (C2) | -7.50 | 2.28 (C2) | -6.40 | 2.16 (C2) |
| **MEOH (1)** | -5.73 | 3.04 (O2) | -6.23 | 2.58 (O2) | -5.70 | 2.84 (O2) |
| **MEOH (2)** | -3.18 | 3.04 (O2) | -6.24 | 2.58 (O2) | -5.72 | 2.84 (O2) |
| **MEOH (3)** | -3.94 | 3.02 (O2) (θ=126) | -4.46 | 2.70 (O2) (θ=128) | — | — |
| **MEOH (4)** | -6.72 | 3.01 (O2) (φ=125) | -4.58 | 2.70 (O2) (φ=128) | — | — |
| **FORM (1)** | -5.45 | 3.09 (O2) (θ=115) | -6.30 | 2.50 (O2) (θ=125) | — | — |
| **FORM (2)** | -4.15 | 3.15 (O2) | -5.75 | 2.62 (O2) | — | — |

**Table 2.** Solute–solvent interaction energies (kcal/mole), equilibrium distances (Å) between solute atom "*X*" and water oxygen atom "OW" (Figure 1), and equilibrium angles (Figure 1) calculated by three different f theoretical methods: *ab initio* Gaussian HF 6–31G(d), QM/MM, and MM. Solute name (e.g. IMID) and water–solute orientation number in column 1 corresponds to the molecular complexes displayed in Figure 1. The experimental interaction energy between water and methoxide has been measured to be –23.9 kcal/mol.[28] The HF 6–31G(d) interaction energies have been scaled by a constant factor of 1.16 for uncharged molecules.[20]

**Table 3**

| Molecule | AM1/MM | | MM (CHARMM22) | |
|---|---|---|---|---|
| (Atom) | ε (kcal) | r* (Å) | ε (kcal) | r* (Å) |
| **IMID, IMIDH (CE, CD, CG)** | -0.0500 | 1.8000 | -0.0500 | 1.8000 |
| **IMID, IMIDH (NE2)** | -0.1000 | 1.7000 | -0.2000 | 1.8500 |
| **IMID, IMIDH (ND)** | -0.1000 | 1.7000 | -0.2000 | 1.8500 |
| **NIC, NICH (C3, C5)** | -0.0100 | 2.1000 | -0.1800 | 1.8000 |
| **NIC, NICH (C4N)** | -0.0001 | 1.5000 | -0.1800 | 1.8000 |
| **NIC, NICH (C10)** | -0.3500 | 2.1000 | -0.1800 | 1.8000 |
| **NIC, NICH (C12)** | -0.1500 | 1.7000 | -0.0700 | 2.0000 |
| **NIC, NICH (N2)** | -0.0330 | 1.8500 | -0.0330 | 1.8500 |
| **NIC, NICH (N14)** | -0.0200 | 1.9000 | -0.0200 | 1.9000 |
| **NIC, NICH (O13)** | -0.1500 | 1.7000 | -0.1200 | 1.7000 |
| **MEO, MEOH FORM (C2)** | -0.0800 | 2.0600 | -0.0800 | 2.0600 |
| **MEO, MEOH FORM (O2)** | -0.0011 | 2.0000 | -0.1200 | 1.7000 |

**Table 3.** The van der Waals parameters of solute for QM/MM and MM (CHARMM) atoms (molecule and atom names correspond to those in Figure 1).

## Table 4:

| *oh(begin)* | *oh(end)* | *hn(begin)* | *hn(end)* | $\Delta G(5)$ | $\Delta G(10)$ | $\Delta G_{rev}(5)$ | $\Delta G_{rev}(10)$ |
|---|---|---|---|---|---|---|---|
| 1.00 | 1.00 | 3.00 | 2.95 | 0.17(0.23) | **0.09(0.23)** | -0.07(0.19) | **-0.07(0.20)** |
| 1.00 | 1.00 | 2.95 | 2.90 | 0.09(0.20) | **0.09(0.20)** | -0.08(0.20) | **-0.03(0.21)** |
| 1.00 | 1.00 | 2.90 | 2.85 | 0.09(0.21) | **0.05(0.21)** | -0.08(0.23) | **-0.08(0.22)** |
| 1.00 | 1.00 | 2.85 | 2.80 | 0.08(0.22) | **0.09(0.22)** | -0.05(0.23) | **-0.04(0.22)** |
| 1.00 | 1.00 | 2.80 | 2.75 | 0.06(0.24) | **0.05(0.23)** | -0.12(0.21) | **-0.09(0.22)** |
| 1.00 | 1.00 | 2.75 | 2.70 | 0.13(0.22) | **0.10(0.22)** | -0.00(0.23) | **-0.10(0.26)** |
| 1.00 | 1.00 | 2.70 | 2.65 | 0.01(0.23) | **0.09(0.27)** | -0.15(0.16) | **-0.22(0.19)** |
| 1.00 | 1.00 | 2.65 | 2.60 | 0.17(0.18) | **0.24(0.22)** | -0.22(0.21) | **-0.18(0.22)** |
| 1.00 | 1.00 | 2.60 | 2.55 | 0.26(0.23) | **0.20(0.25)** | -0.14(0.22) | **-0.14(0.22)** |
| 1.00 | 1.00 | 2.55 | 2.50 | 0.16(0.23) | **0.17(0.23)** | -0.12(0.17) | **-0.16(0.22)** |
| 1.00 | 1.00 | 2.50 | 2.45 | 0.17(0.19) | **0.18(0.23)** | -0.30(0.21) | **-0.28(0.21)** |
| 1.00 | 1.00 | 2.45 | 2.40 | 0.34(0.22) | **0.32(0.22)** | -0.22(0.24) | **-0.24(0.25)** |
| 1.00 | 1.00 | 2.40 | 2.35 | 0.24(0.26) | **0.25(0.27)** | -0.24(0.25) | **-0.25(0.23)** |
| 1.00 | 1.00 | 2.35 | 2.30 | 0.24(0.27) | **0.26(0.25)** | -0.21(0.20) | **-0.25(0.21)** |
| 1.00 | 1.00 | 2.30 | 2.25 | 0.23(0.22) | **0.27(0.23)** | -0.21(0.24) | **-0.21(0.24)** |
| 1.00 | 1.00 | 2.25 | 2.20 | 0.22(0.25) | **0.23(0.25)** | -0.30(0.21) | **-0.25(0.22)** |
| 1.00 | 1.00 | 2.20 | 2.15 | 0.33(0.22) | **0.26(0.24)** | -0.27(0.19) | **-0.23(0.21)** |
| 1.00 | 1.00 | 2.15 | 2.10 | 0.30(0.21) | **0.24(0.23)** | -0.31(0.24) | **-0.37(0.26)** |
| 1.00 | 1.00 | 2.10 | 2.05 | 0.34(0.25) | **0.39(0.28)** | -0.27(0.22) | **-0.27(0.22)** |
| 1.00 | 1.00 | 2.05 | 2.00 | 0.32(0.24) | **0.32(0.24)** | -0.27(0.21) | **-0.31(0.23)** |
| 1.00 | 1.00 | 2.00 | 1.95 | 0.35(0.22) | **0.37(0.24)** | -0.57(0.28) | **-0.53(0.28)** |
| 1.00 | 1.00 | 1.95 | 1.90 | 0.65(0.30) | **0.62(0.29)** | -0.40(0.23) | **-0.35(0.25)** |
| 1.00 | 1.00 | 1.90 | 1.85 | 0.52(0.25) | **0.45(0.26)** | -0.50(0.29) | **-0.50(0.29)** |
| 1.00 | 1.00 | 1.85 | 1.80 | 0.60(0.32) | **0.60(0.32)** | -0.82(0.27) | **-0.80(0.27)** |
| 1.00 | 1.00 | 1.80 | 1.75 | 0.99(0.29) | **0.99(0.29)** | -0.83(0.28) | **-0.86(0.27)** |
| 1.00 | 1.00 | 1.75 | 1.70 | 1.04(0.29) | **1.07(0.28)** | -1.06(0.26) | **-1.03(0.25)** |
| 1.00 | 1.00 | 1.70 | 1.65 | 1.29(0.28) | **1.27(0.27)** | -1.19(0.26) | **-1.21(0.27)** |
| 1.00 | 1.00 | 1.65 | 1.60 | 1.46(0.28) | **1.47(0.29)** | -1.51(0.27) | **-1.50(0.25)** |
| 1.00 | 1.00 | 1.60 | 1.55 | 1.79(0.28) | **1.79(0.26)** | -1.81(0.25) | **-1.80(0.27)** |
| 1.00 | 1.00 | 1.55 | 1.50 | 2.14(0.26) | **2.12(0.27)** | -1.97(0.27) | **-2.04(0.27)** |
| 1.00 | 1.00 | 1.50 | 1.45 | 2.41(0.24) | **2.43(0.24)** | -2.39(0.24) | **-2.43(0.26)** |
| 1.00 | 1.05 | 1.45 | 1.45 | -1.25(0.22) | **-1.32(0.23)** | 1.45(0.24) | **1.37(0.25)** |
| 1.05 | 1.05 | 1.45 | 1.40 | 2.28(0.27) | **2.22(0.27)** | -2.26(0.26) | **-2.31(0.27)** |
| 1.05 | 1.10 | 1.40 | 1.40 | -0.28(0.24) | **-0.29(0.23)** | 0.28(0.25) | **0.30(0.25)** |
| 1.10 | 1.10 | 1.40 | 1.35 | 1.85(0.28) | **1.88(0.26)** | -1.91(0.23) | **-1.86(0.27)** |
| 1.10 | 1.15 | 1.35 | 1.35 | 0.28(0.28) | **0.17(0.31)** | -0.22(0.30) | **-0.22(0.29)** |
| 1.15 | 1.15 | 1.35 | 1.30 | 1.68(0.31) | **1.67(0.32)** | -1.59(0.32) | **-1.65(0.30)** |
| 1.15 | 1.20 | 1.30 | 1.30 | 0.45(0.32) | **0.37(0.32)** | -0.45(0.31) | **-0.52(0.31)** |
| 1.20 | 1.20 | 1.30 | 1.25 | 1.26(0.31) | **1.26(0.30)** | -1.33(0.28) | **-1.34(0.29)** |
| 1.20 | 1.25 | 1.25 | 1.25 | 0.07(0.28) | **0.13(0.30)** | -0.19(0.32) | **-0.11(0.32)** |
| 1.25 | 1.25 | 1.25 | 1.20 | 1.27(0.30) | **1.28(0.30)** | -1.23(0.28) | **-1.17(0.29)** |
| 1.25 | 1.30 | 1.20 | 1.20 | 0.04(0.32) | **-0.07(0.36)** | 0.08(0.33) | **0.10(0.31)** |
| 1.30 | 1.30 | 1.20 | 1.15 | 1.16(0.30) | **1.11(0.31)** | -1.06(0.30) | **-1.05(0.31)** |
| 1.30 | 1.35 | 1.15 | 1.15 | -0.53(0.31) | **-0.55(0.31)** | 0.61(0.33) | **0.59(0.34)** |
| 1.35 | 1.35 | 1.15 | 1.10 | 1.35(0.29) | **1.37(0.28)** | -1.31(0.31) | **-1.32(0.32)** |
| 1.35 | 1.40 | 1.10 | 1.10 | -0.98(0.31) | **-1.05(0.31)** | 1.07(0.32) | **1.06(0.32)** |

| | | | | | | | |
|---|---|---|---|---|---|---|---|
| 1.40 | 1.40 | 1.10 | 1.05 | 2.01(0.31) | **2.05(0.30)** | -2.04(0.29) | **-2.01(0.31)** |
| 1.40 | 1.45 | 1.05 | 1.05 | -1.65(0.34) | **-1.60(0.33)** | 1.62(0.30) | **1.62(0.30)** |
| 1.45 | 1.45 | 1.05 | 1.00 | 3.19(0.31) | **3.20(0.30)** | -3.11(0.31) | **-3.11(0.31)** |
| 1.45 | 1.50 | 1.00 | 1.00 | -2.05(0.33) | **-2.00(0.35)** | 2.25(0.33) | **2.22(0.34)** |
| 1.50 | 1.55 | 1.00 | 1.00 | -2.03(0.33) | **-2.02(0.33)** | 1.83(0.32) | **1.77(0.32)** |
| 1.55 | 1.60 | 1.00 | 1.00 | -1.61(0.32) | **-1.56(0.32)** | 1.65(0.34) | **1.61(0.34)** |
| 1.60 | 1.65 | 1.00 | 1.00 | -1.42(0.33) | **-1.40(0.34)** | 1.65(0.32) | **1.59(0.36)** |
| 1.65 | 1.70 | 1.00 | 1.00 | -1.36(0.32) | **-1.36(0.35)** | 1.40(0.37) | **1.37(0.36)** |
| 1.70 | 1.75 | 1.00 | 1.00 | -1.16(0.36) | **-1.14(0.36)** | 1.15(0.32) | **1.17(0.36)** |
| 1.75 | 1.80 | 1.00 | 1.00 | -0.87(0.32) | **-0.94(0.35)** | 0.91(0.35) | **0.91(0.34)** |
| 1.80 | 1.85 | 1.00 | 1.00 | -0.68(0.35) | **-0.67(0.34)** | 0.68(0.31) | **0.68(0.33)** |
| 1.85 | 1.90 | 1.00 | 1.00 | -0.45(0.31) | **-0.47(0.33)** | 1.10(0.31) | **1.08(0.32)** |
| 1.90 | 1.95 | 1.00 | 1.00 | -0.83(0.29) | **-0.83(0.30)** | 0.44(0.39) | **0.37(0.38)** |
| 1.95 | 2.00 | 1.00 | 1.00 | -0.33(0.37) | **-0.25(0.37)** | 0.37(0.39) | **0.30(0.37)** |
| 2.00 | 2.05 | 1.00 | 1.00 | -0.26(0.37) | **-0.19(0.35)** | 0.13(0.44) | **0.09(0.41)** |
| 2.05 | 2.10 | 1.00 | 1.00 | -0.15(0.42) | **-0.08(0.39)** | 0.13(0.35) | **0.18(0.37)** |
| 2.10 | 2.15 | 1.00 | 1.00 | -0.09(0.35) | **-0.15(0.36)** | 0.29(0.35) | **0.24(0.33)** |
| 2.15 | 2.20 | 1.00 | 1.00 | -0.30(0.36) | **-0.22(0.34)** | 0.06(0.37) | **0.05(0.38)** |
| 2.20 | 2.25 | 1.00 | 1.00 | -0.05(0.37) | **-0.05(0.37)** | 0.00(0.35) | **-0.03(0.34)** |
| 2.25 | 2.30 | 1.00 | 1.00 | 0.03(0.35) | **0.05(0.34)** | 0.10(0.37) | **0.08(0.38)** |
| 2.30 | 2.35 | 1.00 | 1.00 | -0.10(0.35) | **-0.09(0.37)** | 0.06(0.40) | **0.04(0.40)** |
| 2.35 | 2.40 | 1.00 | 1.00 | -0.09(0.40) | **-0.06(0.39)** | 0.26(0.37) | **0.28(0.35)** |
| 2.40 | 2.45 | 1.00 | 1.00 | -0.24(0.36) | **-0.24(0.35)** | 0.14(0.39) | **0.11(0.39)** |
| 2.45 | 2.50 | 1.00 | 1.00 | -0.15(0.38) | **-0.12(0.38)** | 0.16(0.36) | **0.16(0.35)** |
| | | | | **15.23** | **15.11** | **-13.49** | **-14.16** |

**Table 4.** Symbol "*oh*" (columns 1 and 2) denotes the proton reaction coordinate *d(O2 – H2);* symbol "*hn*" denotes the proton reaction coordinate *d(H2 – NE2)* (Figure 2). "*Begin*" (columns 1 and 3) means initial value of the reaction coordinates before perturbation, and "*end*" (columns 2 and 4) means the final value of reaction coordinates after the perturbation (i.e., reaction coordinates are perturbed from *oh(begin)* and *hn(begin)* to *oh(end)* and *hn(end)*). Units of all reaction coordinates are in Å. $\Delta G(5)$ and $\Delta G(10)$ are forward free energy changes for a perturbation window after averaging 5000 and 10000 steps of data collection, respectively. $\Delta G_{rev}(5)$ and $\Delta G_{rev}(10)$ are the free energy changes after averaging 5000 and 10000 data collection steps for the reverse perturbation in the window concerned. $\Delta G$ ( $\Delta G_{rev}$ ) values for each window are shown with fluctuations in parentheses. Units of all free energies are in kcal/mole. For each perturbation, the system is first equilibrated for 20 ps (1 fs MD time steps) with reaction coordinates fixed (using SHAKE) at values *oh(begin)* and *hn(begin).* The free energies in the forward direction are calculated by perturbing reaction coordinates from *oh(begin)* and *hn(begin)* to *oh(end)* and *hn(end).* For each backward perturbation, $\Delta G_{rev}$ is calculated by perturbing reaction coordinates from *oh(end)* and *hn(end)* to *oh(begin)* and *hn(begin).* The last row displays the net free energy change summed over all perturbation windows.

**Table 5**

| *ch(begin)* | *ch(end)* | *hc(begin)* | *hc(end)* | $\Delta G(5)$ | $\Delta G(10)$ | $\Delta G_{rev}(5)$ | $\Delta G_{rev}(10)$ |
|---|---|---|---|---|---|---|---|
| 1.10 | 1.10 | 3.10 | 3.05 | -0.00(0.34) | **-0.03(0.34)** | 0.04(0.35) | **0.05(0.36)** |
| 1.10 | 1.10 | 3.05 | 3.00 | -0.07(0.33) | **-0.07(0.34)** | 0.03(0.33) | **-0.01(0.36)** |
| 1.10 | 1.10 | 3.00 | 2.95 | -0.02(0.31) | **0.01(0.35)** | -0.02(0.37) | **-0.04(0.37)** |
| 1.10 | 1.10 | 2.95 | 2.90 | 0.03(0.37) | **0.06(0.37)** | -0.01(0.38) | **-0.01(0.38)** |
| 1.10 | 1.10 | 2.90 | 2.85 | 0.01(0.36) | **0.01(0.37)** | -0.09(0.37) | **-0.07(0.37)** |
| 1.10 | 1.10 | 2.85 | 2.80 | 0.13(0.35) | **0.11(0.35)** | -0.01(0.40) | **-0.01(0.38)** |
| 1.10 | 1.10 | 2.80 | 2.75 | -0.01(0.39) | **0.02(0.37)** | -0.02(0.38) | **-0.01(0.39)** |
| 1.10 | 1.10 | 2.75 | 2.70 | 0.05(0.37) | **0.04(0.37)** | -0.02(0.36) | **-0.03(0.38)** |
| 1.10 | 1.10 | 2.70 | 2.65 | 0.04(0.36) | **0.04(0.37)** | -0.09(0.40) | **-0.11(0.40)** |
| 1.10 | 1.10 | 2.65 | 2.60 | 0.10(0.38) | **0.13(0.38)** | -0.06(0.40) | **-0.05(0.39)** |
| 1.10 | 1.10 | 2.60 | 2.55 | 0.06(0.38) | **0.06(0.38)** | -0.16(0.39) | **-0.18(0.38)** |
| 1.10 | 1.10 | 2.55 | 2.50 | 0.21(0.38) | **0.23(0.37)** | -0.13(0.35) | **-0.11(0.38)** |
| 1.10 | 1.10 | 2.50 | 2.45 | 0.19(0.34) | **0.15(0.37)** | -0.06(0.34) | **-0.14(0.38)** |
| 1.10 | 1.10 | 2.45 | 2.40 | 0.13(0.33) | **0.18(0.37)** | -0.23(0.34) | **-0.24(0.36)** |
| 1.10 | 1.10 | 2.40 | 2.35 | 0.29(0.37) | **0.30(0.38)** | -0.11(0.33) | **-0.09(0.35)** |
| 1.10 | 1.10 | 2.35 | 2.30 | 0.17(0.34) | **0.16(0.35)** | -0.39(0.41) | **-0.29(0.40)** |
| 1.10 | 1.10 | 2.30 | 2.25 | 0.46(0.41) | **0.41(0.39)** | -0.32(0.38) | **-0.31(0.39)** |
| 1.10 | 1.10 | 2.25 | 2.20 | 0.39(0.38) | **0.37(0.39)** | -0.41(0.38) | **-0.39(0.36)** |
| 1.10 | 1.10 | 2.20 | 2.15 | 0.51(0.38) | **0.51(0.36)** | -0.49(0.38) | **-0.48(0.38)** |
| 1.10 | 1.10 | 2.15 | 2.10 | 0.59(0.37) | **0.58(0.37)** | -0.59(0.38) | **-0.56(0.39)** |
| 1.10 | 1.10 | 2.10 | 2.05 | 0.69(0.36) | **0.65(0.37)** | -0.63(0.35) | **-0.62(0.34)** |
| 1.10 | 1.10 | 2.05 | 2.00 | 0.77(0.34) | **0.78(0.33)** | -0.91(0.40) | **-0.89(0.38)** |
| 1.10 | 1.10 | 2.00 | 1.95 | 1.00(0.41) | **1.01(0.38)** | -0.86(0.36) | **-0.84(0.36)** |
| 1.10 | 1.10 | 1.95 | 1.90 | 1.00(0.35) | **0.99(0.35)** | -1.02(0.40) | **-0.95(0.40)** |
| 1.10 | 1.10 | 1.90 | 1.85 | 1.13(0.39) | **1.07(0.39)** | -1.17(0.37) | **-1.13(0.39)** |
| 1.10 | 1.10 | 1.85 | 1.80 | 1.35(0.36) | **1.29(0.38)** | -1.39(0.40) | **-1.35(0.40)** |
| 1.10 | 1.10 | 1.80 | 1.75 | 1.56(0.40) | **1.51(0.40)** | -1.45(0.39) | **-1.46(0.39)** |
| 1.10 | 1.10 | 1.75 | 1.70 | 1.66(0.39) | **1.66(0.38)** | -1.48(0.39) | **-1.50(0.39)** |
| 1.10 | 1.10 | 1.70 | 1.65 | 1.71(0.38) | **1.73(0.38)** | -1.73(0.39) | **-1.77(0.40)** |
| 1.10 | 1.10 | 1.65 | 1.60 | 1.98(0.40) | **2.01(0.40)** | -2.06(0.42) | **-2.05(0.29)** |
| 1.10 | 1.10 | 1.60 | 1.55 | 2.24(0.43) | **2.23(0.41)** | -2.28(0.39) | **-2.27(0.39)** |
| 1.10 | 1.15 | 1.55 | 1.55 | -1.59(0.37) | **-1.61(0.37)** | 1.72(0.38) | **1.73(0.38)** |
| 1.15 | 1.15 | 1.55 | 1.50 | 2.01(0.51) | **2.03(0.48)** | -1.93(0.49) | **-1.94(0.48)** |
| 1.15 | 1.20 | 1.50 | 1.50 | -0.65(0.46) | **-0.56(0.45)** | 0.44(0.44) | **0.46(0.43)** |
| 1.20 | 1.20 | 1.50 | 1.45 | 1.89(0.52) | **1.73(0.54)** | -1.72(0.51) | **-1.67(0.55)** |
| 1.20 | 1.25 | 1.45 | 1.45 | 0.21(0.46) | **0.19(0.47)** | 0.15(0.50) | **0.06(0.52)** |
| 1.25 | 1.25 | 1.45 | 1.40 | 1.00(0.63) | **1.15(0.69)** | -0.67(0.61) | **-0.68(0.59)** |
| 1.25 | 1.30 | 1.40 | 1.40 | -0.34(0.59) | **-0.23(0.56)** | 0.86(0.51) | **0.82(0.54)** |
| 1.30 | 1.30 | 1.40 | 1.35 | -0.59(0.56) | **-0.55(0.61)** | 0.86(0.56) | **0.90(0.54)** |
| 1.30 | 1.35 | 1.35 | 1.35 | -1.55(0.59) | **-1.46(0.56)** | 1.46(0.54) | **1.43(0.54)** |
| 1.35 | 1.35 | 1.35 | 1.30 | -1.20(0.46) | **-1.26(0.47)** | 1.18(0.45) | **1.19(0.47)** |
| 1.35 | 1.40 | 1.30 | 1.30 | -1.67(0.48) | **-1.79(0.50)** | 1.87(0.44) | **1.85(0.49)** |
| 1.40 | 1.40 | 1.30 | 1.25 | -1.26(0.41) | **-1.22(0.44)** | 1.33(0.45) | **1.33(0.45)** |
| 1.40 | 1.45 | 1.25 | 1.25 | -2.05(0.46) | **-2.10(0.44)** | 2.38(0.35) | **2.41(0.34)** |
| 1.45 | 1.45 | 1.25 | 1.20 | -0.93(0.33) | **-0.93(0.35)** | 0.99(0.34) | **0.97(0.33)** |
| 1.45 | 1.50 | 1.20 | 1.20 | -2.19(0.36) | **-2.19(0.37)** | 2.24(0.33) | **2.22(0.33)** |

| | | | | | | | |
|---|---|---|---|---|---|---|---|
| 1.50 | 1.50 | 1.20 | 1.15 | 0.07(0.30) | **0.06(0.30)** | -0.01(0.30) | **-0.02(0.31)** |
| 1.50 | 1.55 | 1.15 | 1.15 | -2.07(0.32) | **-2.07(0.31)** | 2.29(0.31) | **2.33(0.31)** |
| 1.55 | 1.55 | 1.15 | 1.10 | 1.31(0.29) | **1.31(0.28)** | -1.16(0.28) | **-1.17(0.28)** |
| 1.55 | 1.60 | 1.10 | 1.10 | -2.09(0.29) | **-2.09(0.28)** | 2.15(0.26) | **2.12(0.27)** |
| 1.60 | 1.65 | 1.10 | 1.10 | -1.80(0.24) | **-1.79(0.27)** | 1.83(0.31) | **1.83(0.30)** |
| 1.65 | 1.70 | 1.10 | 1.10 | -1.58(0.29) | **-1.56(0.28)** | 1.58(0.23) | **1.62(0.23)** |
| 1.70 | 1.75 | 1.10 | 1.10 | -1.32(0.22) | **-1.37(0.22)** | 1.36(0.23) | **1.33(0.23)** |
| 1.75 | 1.80 | 1.10 | 1.10 | -1.14(0.22) | **-1.12(0.22)** | 1.18(0.25) | **1.16(0.25)** |
| 1.80 | 1.85 | 1.10 | 1.10 | -1.02(0.25) | **-1.01(0.24)** | 1.01(0.27) | **1.01(0.26)** |
| 1.85 | 1.90 | 1.10 | 1.10 | -0.89(0.27) | **-0.87(0.26)** | 0.87(0.27) | **0.92(0.29)** |
| 1.90 | 1.95 | 1.10 | 1.10 | -0.75(0.26) | **-0.82(0.28)** | 0.79(0.21) | **0.78(0.22)** |
| 1.95 | 2.00 | 1.10 | 1.10 | -0.65(0.20) | **-0.65(0.21)** | 0.77(0.24) | **0.74(0.23)** |
| 2.00 | 2.05 | 1.10 | 1.10 | -0.66(0.24) | **-0.63(0.23)** | 0.58(0.21) | **0.60(0.22)** |
| 2.05 | 2.10 | 1.10 | 1.10 | -1.16(0.22) | **-0.93(0.23)** | 0.55(0.22) | **0.52(0.24)** |
| 2.10 | 2.15 | 1.10 | 1.10 | -0.43(0.21) | **-0.42(0.23)** | 0.48(0.22) | **0.50(0.24)** |
| 2.15 | 2.20 | 1.10 | 1.10 | -0.38(0.21) | **-0.42(0.23)** | 0.35(0.24) | **0.37(0.24)** |
| 2.20 | 2.25 | 1.10 | 1.10 | -0.27(0.24) | **-0.29(0.23)** | 0.27(0.28) | **0.34(0.30)** |
| 2.25 | 2.30 | 1.10 | 1.10 | -0.23(0.27) | **-0.30(0.29)** | 0.31(0.22) | **0.25(0.24)** |
| 2.30 | 2.35 | 1.10 | 1.10 | -0.21(0.21) | **-0.18(0.23)** | 0.19(0.23) | **0.21(0.23)** |
| 2.35 | 2.40 | 1.10 | 1.10 | -0.13(0.22) | **-0.15(0.22)** | 0.19(0.25) | **0.17(0.26)** |
| 2.40 | 2.45 | 1.10 | 1.10 | -0.13(0.23) | **-0.13(0.25)** | 0.25(0.23) | **0.21(0.24)** |
| 2.45 | 2.50 | 1.10 | 1.10 | -0.19(0.23) | **-0.16(0.23)** | 0.11(0.23) | **0.09(0.22)** |
| 2.50 | 2.55 | 1.10 | 1.10 | -0.06(0.23) | **-0.04(0.22)** | 0.10(0.24) | **0.09(0.24)** |
| 2.55 | 2.60 | 1.10 | 1.10 | -0.06(0.23) | **-0.06(0.24)** | 0.09(0.23) | **0.06(0.23)** |
| 2.60 | 2.65 | 1.10 | 1.10 | -0.07(0.23) | **-0.04(0.23)** | -0.04(0.24) | **-0.03(0.22)** |
| 2.65 | 2.70 | 1.10 | 1.10 | 0.03(0.23) | **0.04(0.21)** | 0.02(0.21) | **0.03(0.23)** |
| 2.70 | 2.75 | 1.10 | 1.10 | 0.01(0.22) | **-0.01(0.23)** | -0.02(0.21) | **-0.01(0.22)** |
| 2.75 | 2.80 | 1.10 | 1.10 | 0.04(0.21) | **0.04(0.22)** | -0.06(0.23) | **-0.08(0.23)** |
| | | | | -6.40 | **-6.30** | 9.07 | **9.10** |

**Table 5:** "*ch*" (columns 1 and 2) denotes hydride reaction coordinate *d(C2 – H21), and* symbol "*hc*" denotes hydride reaction coordinate *d(H21 – C4N)* (see Figure 3). "*Begin*" (columns 1 and 3) means the initial value of reaction coordinates before the perturbation, and "*end*" (columns 2 and 4) refers to the final value of reaction coordinates after the perturbation (i.e., reaction coordinates are perturbed from *ch(begin)* and *hc(begin)* to *ch(end)* and *hc(end)*). The units and simulation procedure are the same as described in Table 4. The free energies in the forward direction are calculated by perturbing reaction coordinates from *ch(begin)* and *hc(begin)* to *ch(end)* and *hc(end)*. For each perturbation in the reverse direction, $\Delta G_{rev}$ is calculated by perturbing reaction coordinates from *ch(end)* and *hc(end)* to *ch(begin)* and *hc(begin)*.

**Chemical Formula 1** (for page 3 of this manuscript). L.L. Ho, A.D. MacKerell, Jr., and P.A. Bash; "Proton and Hydride Transfers in Solution: Hybrid QM/MM Free Energy Perturbation Study".

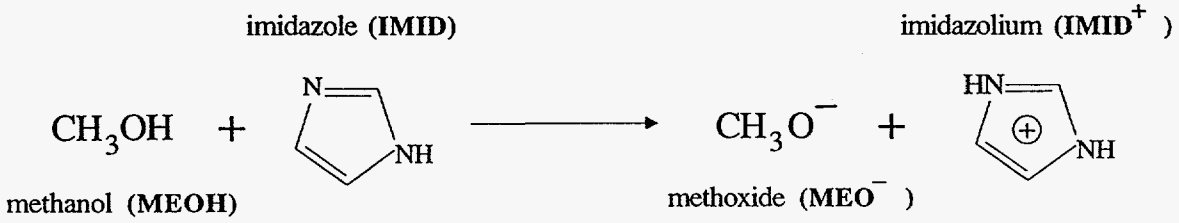

**Chemical Formula 2** (for page 3 of this manuscript). L.L. Ho, A.D. MacKerell, Jr., and P.A. Bash; "Proton and Hydride Transfers in Solution: Hybrid QM/MM Free Energy Perturbation Study".

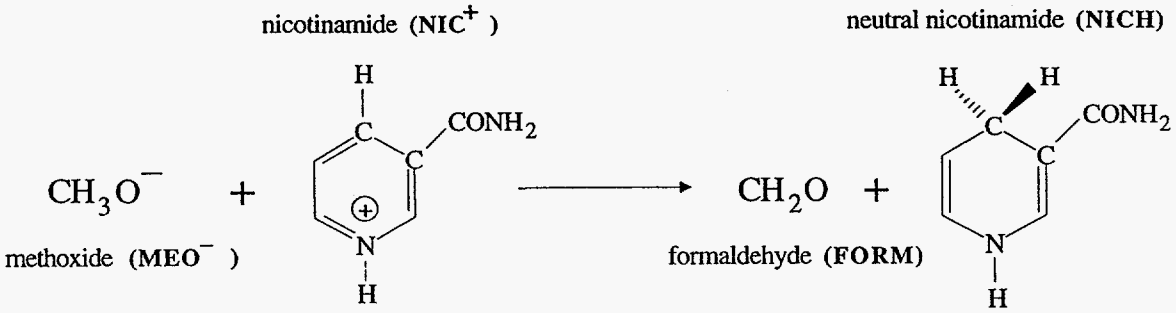

**Figure 1.** Solute–solvent complexes for QM/MM interaction energy calibrations

**Figure 2.** Schematic diagram of the proton transfer (**R1**) solute. The proton is the atom labeled "H2", and the two proton reaction coordinates are the vectors labeled **d(O2–H2)** and **d(H2–NE2)**.

**Figure 3.** Schematic diagram of the hydride transfer (**R2**) solute. The hydride is the atom labeled "H21", and the two hydride reaction coordinates are the vectors labeled **d(C2–H21)** and **d(H21–C4N)**.

**Figure 4.** Free energy "profile" for the proton transfer reaction listed in Table 4. The points along the ordinate correspond to the reaction coordinates. The abscissa gives the cumulative free energies along this reaction coordinate for the forward (——) and reverse directions (– – –). The difference in the free energies between the points A and B is the calculated free energy change for the proton transfer reaction.

**Figure 5.** Free energy "profile" for the hydride transfer reaction listed in Table 5. The points along the ordinate correspond to the reaction coordinates. The abscissa gives the accumulative free energies along this reaction coordinate for the forward (——) and reverse directions (– – –). The difference in the free energies between the points A and B is the calculated free energy change for the hydride transfer reaction.

**Figure 1** (**Figure 1a** to **Figure 1g**) L.L. Ho, A.D. MacKerell, Jr., and P.A. Bash; "Proton and Hydride Transfers in Solution: Hybrid QM/MM Free Energy Perturbation Study".

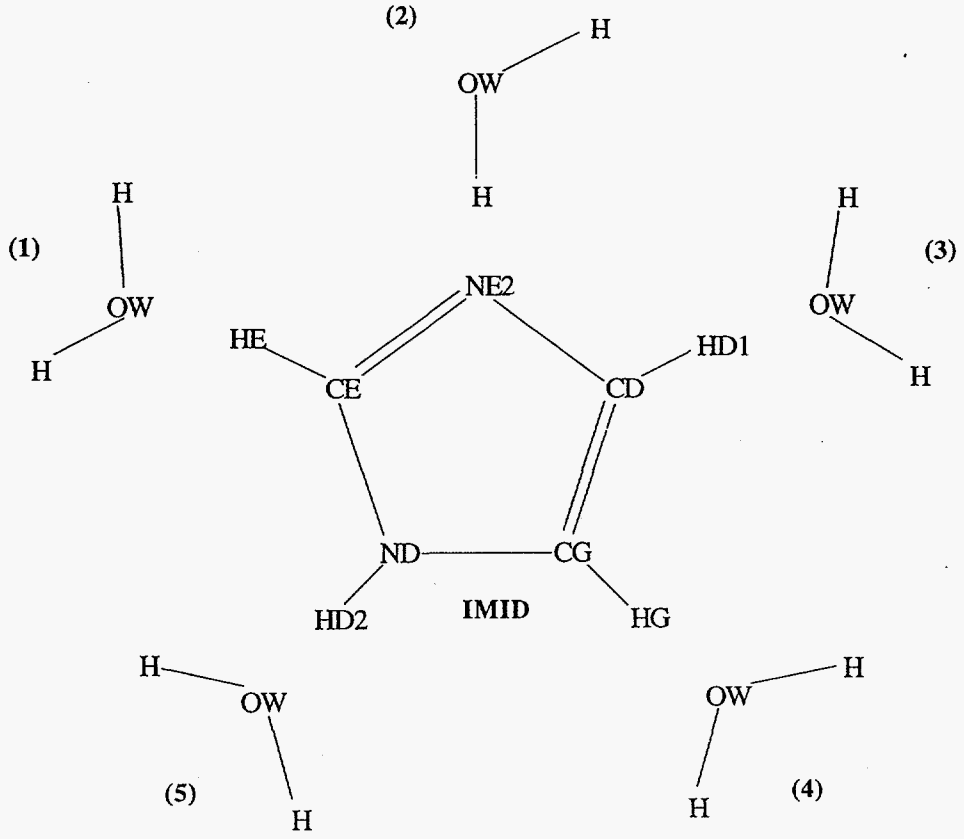


**1a**

**Figure 1** (**Figure 1a** to **Figure 1g**) L.L. Ho, A.D. MacKerell, Jr., and P.A. Bash; "Proton and Hydride Transfers in Solution: Hybrid QM/MM Free Energy Perturbation Study".

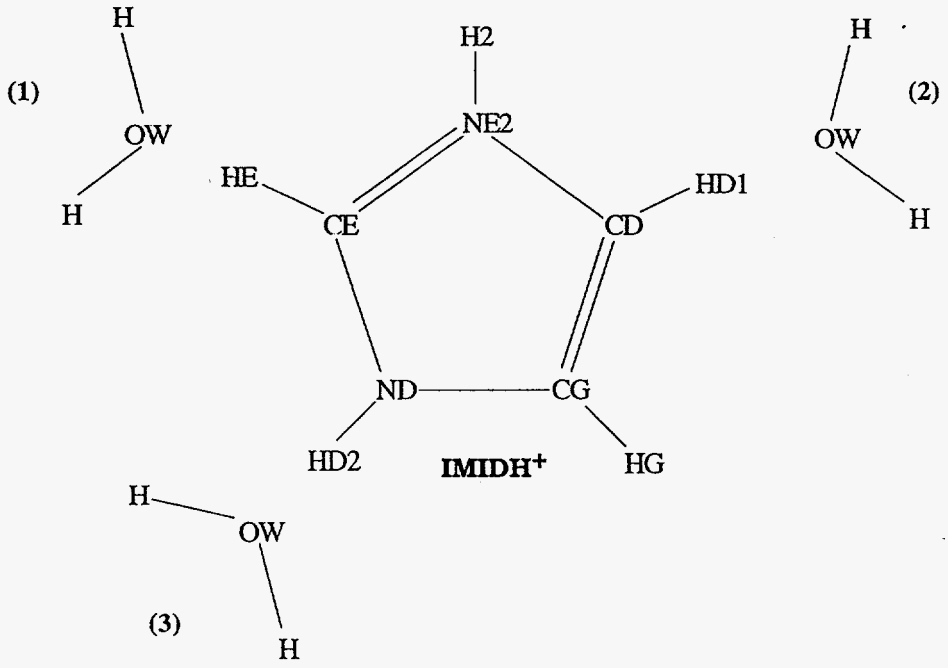


**1b**

**Figure 1** (**Figure 1a** to **Figure 1g**) L.L. Ho, A.D. MacKerell, Jr., and P.A. Bash; "Proton and Hydride Transfers in Solution: Hybrid QM/MM Free Energy Perturbation Study".

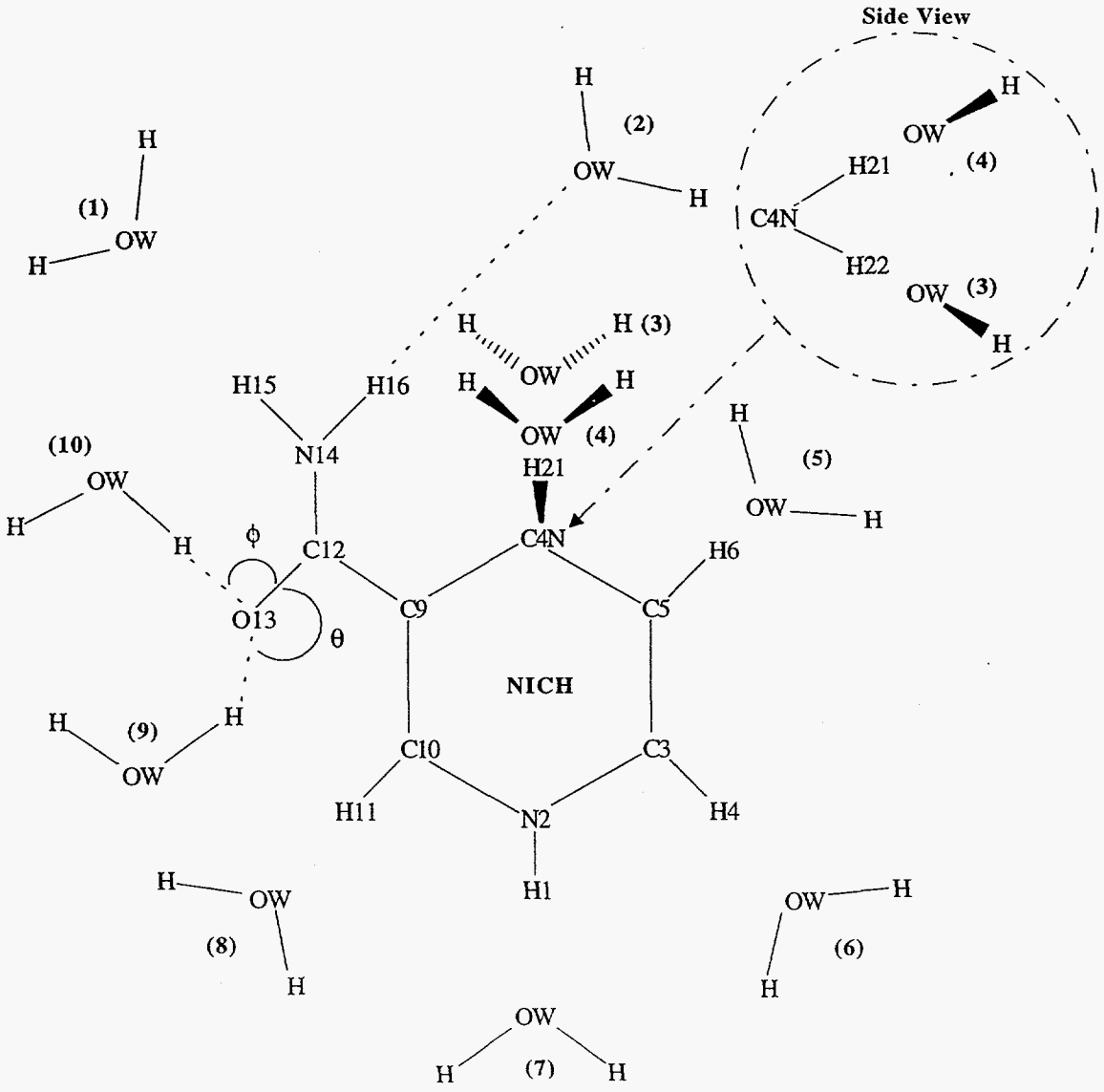


**1c**

**Figure 1 (Figure 1a to Figure 1g)** L.L. Ho, A.D. MacKerell, Jr., and P.A. Bash; "Proton and Hydride Transfers in Solution: Hybrid QM/MM Free Energy Perturbation Study".

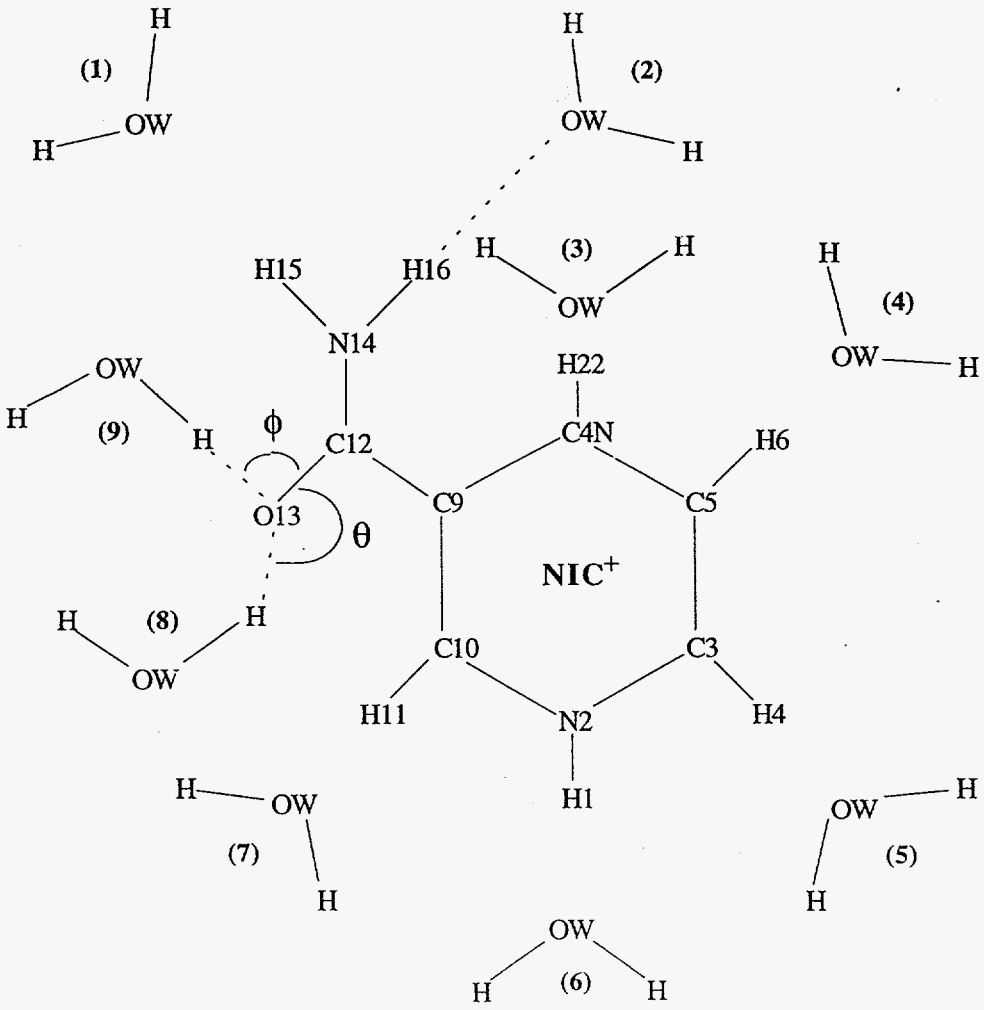


**1d**

**Figure 1** (**Figure 1a** to **Figure 1g**) L.L. Ho, A.D. MacKerell, Jr., and P.A. Bash; "Proton and Hydride Transfers in Solution: Hybrid QM/MM Free Energy Perturbation Study".

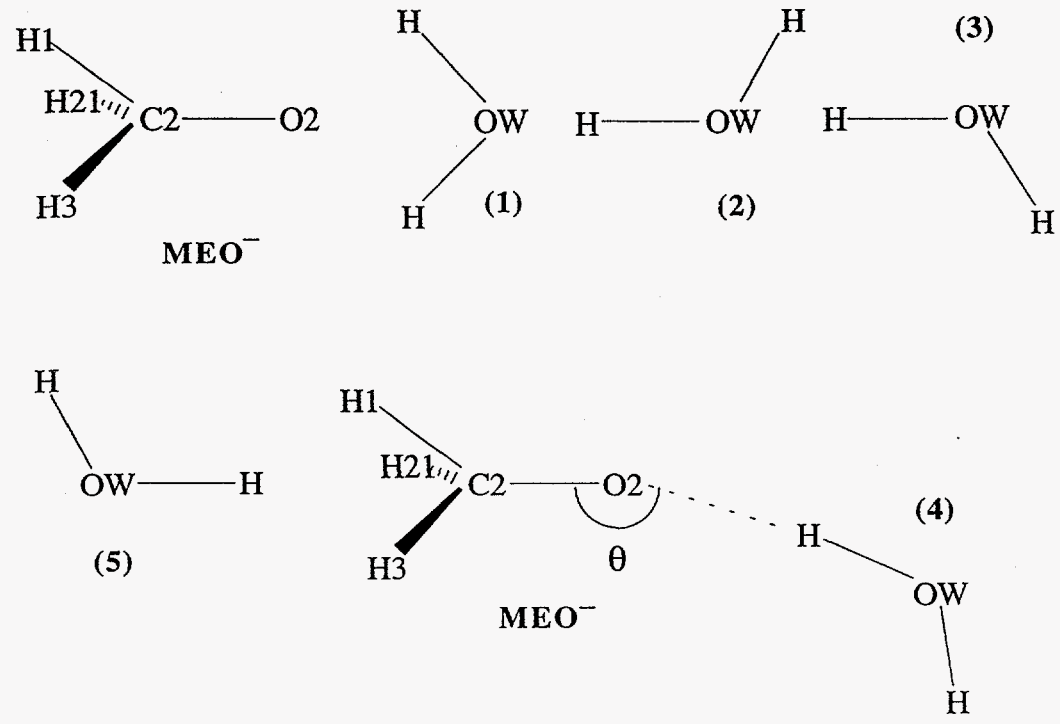


**1e**

**Figure 1** (**Figure 1a** to **Figure 1g**) L.L. Ho, A.D. MacKerell, Jr., and P.A. Bash; "Proton and Hydride Transfers in Solution: Hybrid QM/MM Free Energy Perturbation Study".

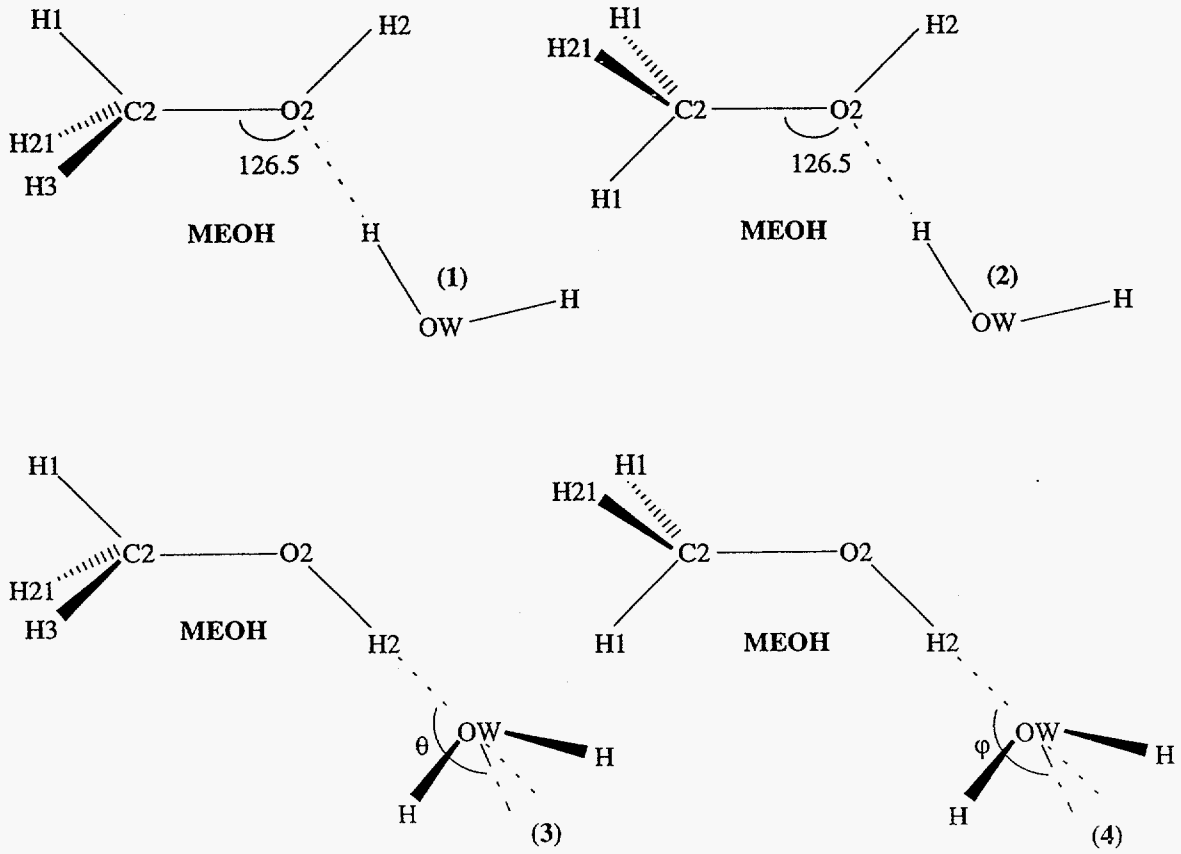


**1f**

**Figure 1** (**Figure 1a** to **Figure 1g**) L.L. Ho, A.D. MacKerell, Jr., and P.A. Bash; "Proton and Hydride Transfers in Solution: Hybrid QM/MM Free Energy Perturbation Study".

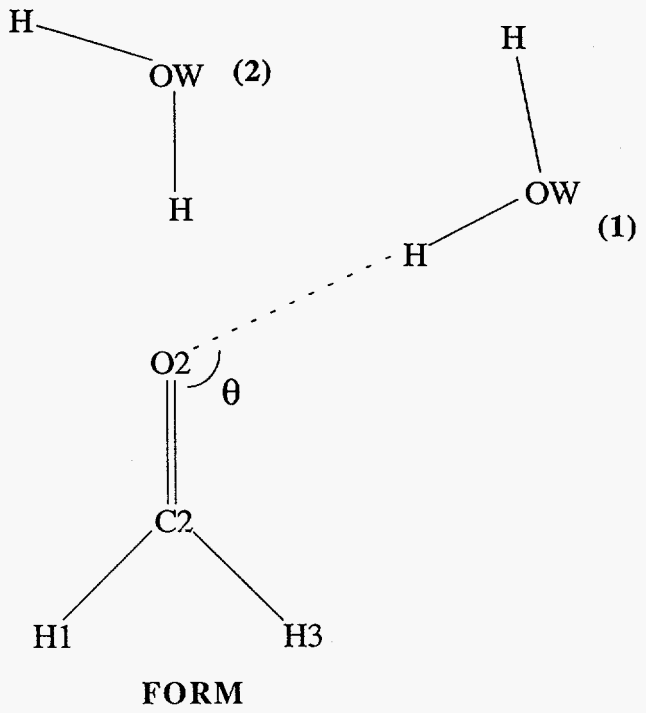


**1g**

**Figure 2** L.L. Ho, A.D. MacKerell, Jr., and P.A. Bash; "Proton and Hydride Transfers in Solution: Hybrid QM/MM Free Energy Perturbation Study".

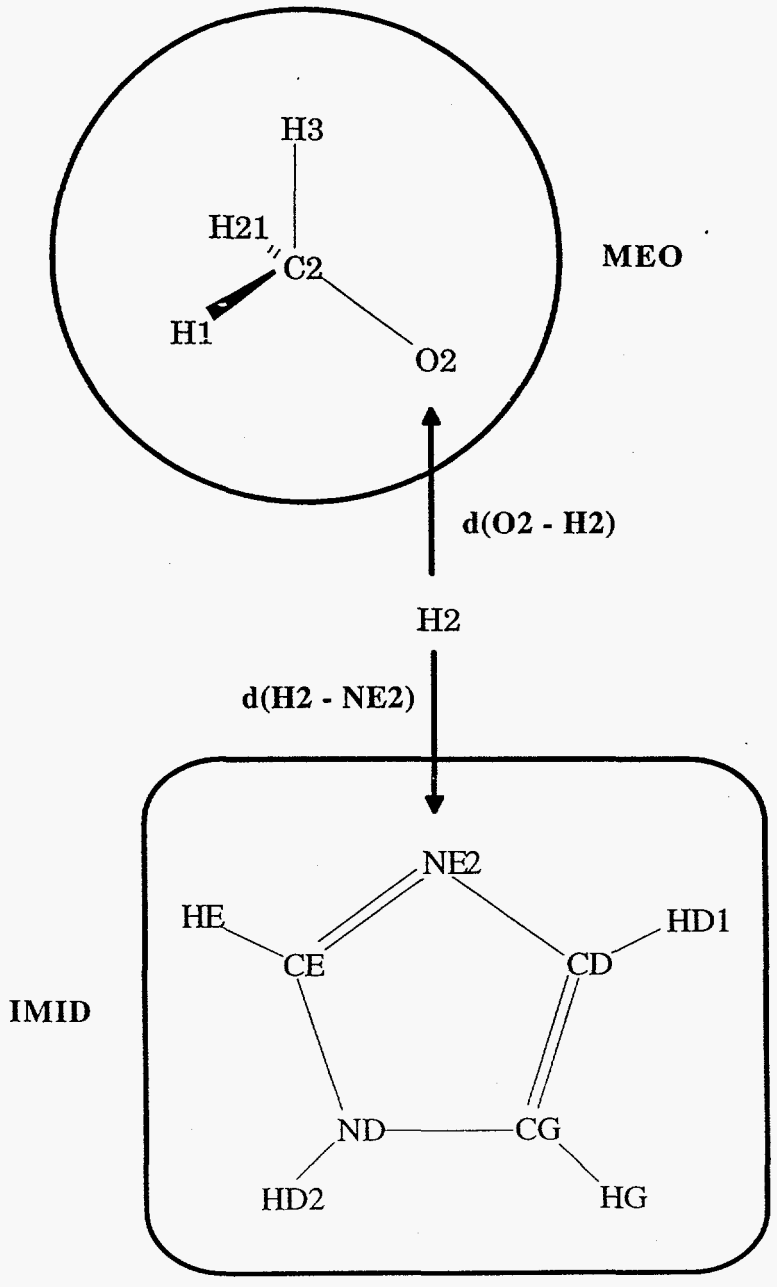

**Figure 3** L.L. Ho, A.D. MacKerell, Jr., and P.A. Bash; "Proton and Hydride Transfers in Solution: Hybrid QM/MM Free Energy Perturbation Study".

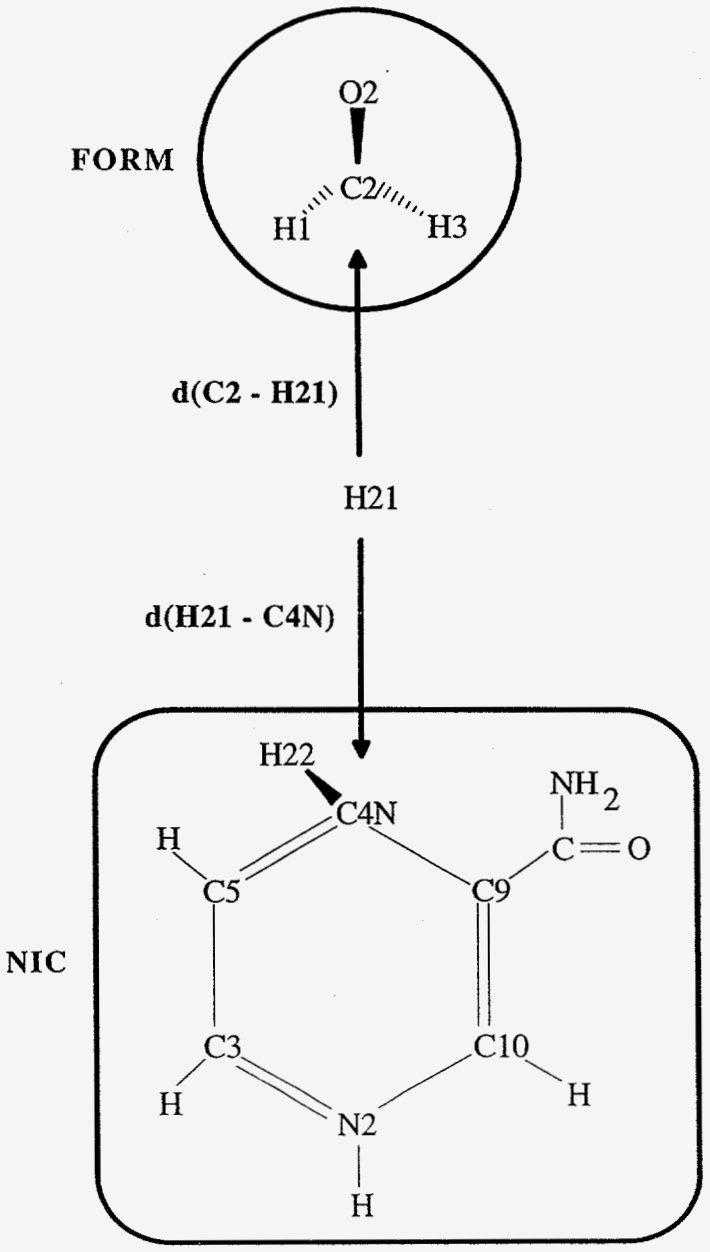

**Figure 4** L.L. Ho, A.D. MacKerell, Jr., and P.A. Bash; "Proton and Hydride Transfers in Solution: Hybrid QM/MM Free Energy Perturbation Study".

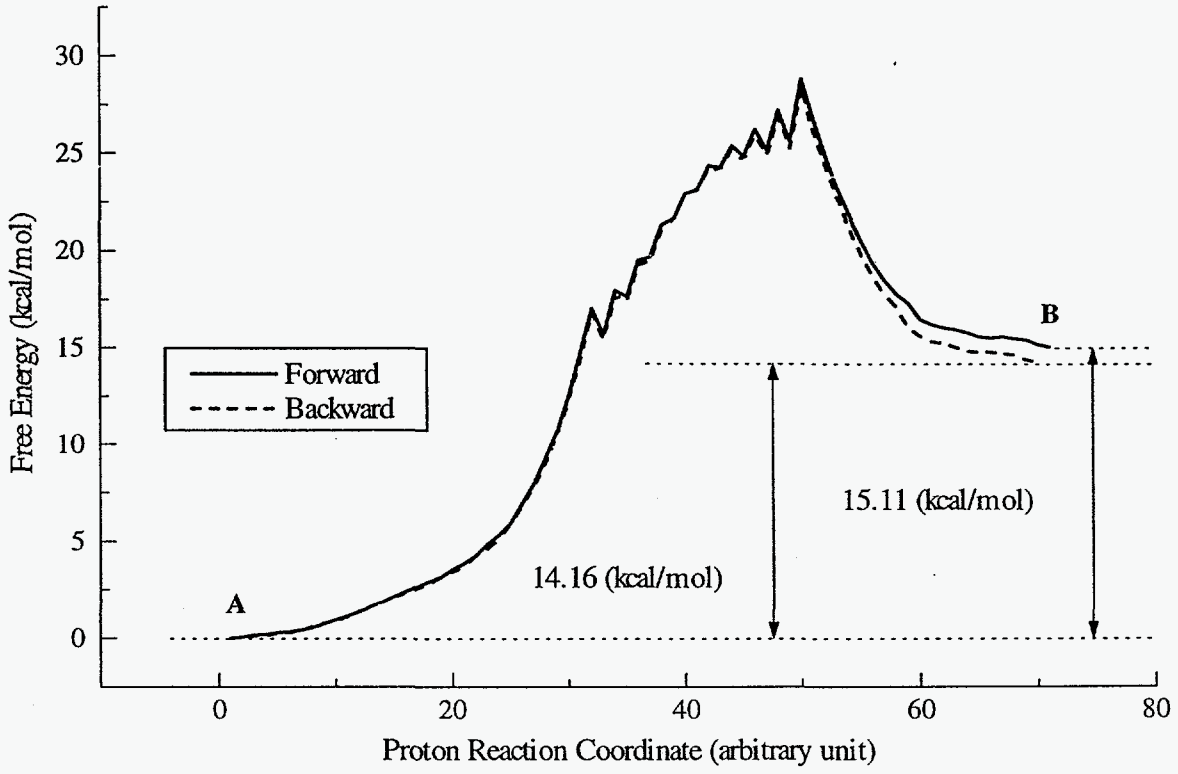

**Figure 5** L.L. Ho, A.D. MacKerell, Jr., and P.A. Bash; "Proton and Hydride Transfers in Solution: Hybrid QM/MM Free Energy Perturbation Study".